Geophysical Research Letters

RESEARCH LETTER
10.1029/2021GL095485

How Many Types of Severe Hailstorm Environments Are There Globally?

Ziwei Zhou[1], Qinghong Zhang[1], John T. Allen[2], Xiang Ni[3], and Chan-Pang Ng[1]

[1]Department of Atmospheric and Oceanic Sciences, School of Physics, Peking University, Beijing, China, [2]Department of Earth and Atmospheric Sciences, Central Michigan University, Mount Pleasant, MI, USA, [3]School of Geographical Sciences, Southwest University, Chongqing, China

Key Points:

- Artificial intelligence clustering identifies five distinctive severe hailstorms environmental conditions derived from Global Precipitation Measurement satellite
- The environmental conditions reflect a consistent relationship between instability, melting level height, and vertical wind shear
- Multiple environment types pose challenges for modeling present frequency and anticipating the response of hail to climate change

Supporting Information:

Supporting Information may be found in the online version of this article.

Correspondence to:

Q. Zhang and J. T. Allen,
qzhang@pku.edu.cn;
allen4jt@cmich.edu

Citation:

Zhou, Z., Zhang, Q., Allen, J. T., Ni, X., & Ng, C.-P. (2021). How many types of severe hailstorm environments are there globally? *Geophysical Research Letters*, *48*, e2021GL095485. https://doi.org/10.1029/2021GL095485

Received 29 JUL 2021
Accepted 26 NOV 2021

Author Contributions:

Conceptualization: Qinghong Zhang, John T. Allen
Data curation: Qinghong Zhang, Xiang Ni
Formal analysis: Ziwei Zhou
Investigation: Ziwei Zhou
Methodology: Ziwei Zhou, Chan-Pang Ng
Resources: Qinghong Zhang
Software: Ziwei Zhou
Supervision: Qinghong Zhang
Validation: Ziwei Zhou
Visualization: Ziwei Zhou

Abstract Understanding how severe hailstorms will respond to climate change remains challenging partially due to an incomplete understanding of how different environments produce hail. Leveraging a record of 14,297 global potential severe hailstorms detected by spaceborne precipitation radar, here for the first time, we explore global differences in the five distinct environmental types producing these storms. Two are found over tropical plains and hills with high convective instability, high-moderate moisture, and low vertical wind shear (VWS). The third type are supercell environments characterized by strong VWS, with moderate instability and moisture, commonly occurring over mid-latitude plains. Higher latitude plains and elevated terrain reflect the final two, with moderate VWS and low melting height, instability, and moisture. The variety of hailstorm environment types illustrates distinctions in the associated convective mode and embryo type, highlighting that multiple environment types pose challenges for modeling present frequency and anticipating the response of hail to climate change.

Plain Language Summary The impacts of climate change on the global occurrence of hailstorms are full of uncertainty, which partially results from an incomplete understanding of hail-producing environmental conditions. However, a fundamental limitation of these prior approaches is the use of a single metric or formative mechanism to consider hail occurrence. Leveraging a combination of satellite detection and artificial intelligence clustering method, this research for the first time demonstrates that there are five distinct environmental conditions producing severe hailstorms globally. The different global environmental characteristics obey a consistent relationship between variables, balancing between unstable conditions, melting level height, and the vertical wind shear. A key finding is that the variety of hailstorm environment types illustrates distinctions in the associated convective mode and possibly embryo type, highlighting that considering only one hailstorm environmental condition is unlikely to capture how these individual environment types respond to climate change.

1. Introduction

How hailstorm occurrence will change in response to the warming climate is a hot topic, however the consensus regarding future projected changes is uncertain (Raupach et al., 2021; Seneviratne et al., 2012). This uncertainty results from the lack of uniform hail reporting to understand the present occurrence, and weaknesses in the physical linkage between hailstorms and the background atmospheric environment (Allen et al., 2020; Brimelow et al., 2017; Mahoney, 2020; Mahoney et al., 2012; Punge & Kunz, 2016). Due to the high computational costs and large uncertainty of physical parameterization of dynamic numerical simulations that are capable of resolving hail (e.g., Adams-Selin & Ziegler, 2016; Brimelow et al., 2002), empirical parameters to distinguish the environments of significant severe thunderstorms have been a typical approach to anticipate severe hailstorm occurrence (Brooks et al., 2003; Czernecki et al., 2019; Prein & Holland, 2018; Taszarek, Allen, et al., 2021). Many regional studies have explored statistical environmental relationships for hailstorms (Allen et al., 2015; Groenemeijer & van Delden, 2007; Johnson & Sugden, 2014; Kahraman et al., 2016; Ma et al., 2021; Manzato, 2013; Prein & Holland, 2018; Púčik et al., 2015), but this regional focus has left the global picture of how hail is related to atmospheric predicands unclear. Another complicating factor when characterizing hailstorms between different regions is that the data available to identify hail have significant differences in spatio-temporal resolution, and there are biases between the reanalysis datasets and observations used (Punge & Kunz, 2016; Taszarek, Pilguj, et al., 2021). To address this gap and circumvent the limitations of the observed records, satellite-based detections

Writing – original draft: Ziwei Zhou
Writing – review & editing: Qinghong Zhang, John T. Allen

of hailstorms from empirical algorithms can be used to provide a spatiotemporally consistent record of these events (e.g., Ni et al., 2017).

Hailstorm environments are challenging to define in part because of the myriad of processes that result in the production of these phenomena (Brimelow et al., 2017). Hailstones form in thunderstorms with strong updrafts, which allow hailstone embryos to grow by accretion. The hailstone embryo can be divided into two types, graupel and frozen droplets (Knight & Knight, 1974). These hailstone embryos are entrained into the updraft and mainly collide with supercooled droplets which freeze, the result of many such collisions being hailstone growth. When hailstones are too large to be sustained aloft by the updraft or move outside its periphery they begin to fall. Melting begins as ice particles fall below the melting level, with higher levels and more moist sub-cloud air accelerating the melting process, which has a greater impact on small hail (Brimelow et al., 2017; Dessens et al., 2015; Mahoney et al., 2012; Pruppacher & Klett, 1997; R. M. Rasmussen & Heymsfield, 1987; Willis & Heymsfield, 1989). Stronger and longer-lived updrafts are also known to provide favorable conditions for the growth of large hailstones (Dennis & Kumjian, 2017; Gutierrez & Kumjian, 2021; Nelson, 1983, 1987). Strong vertical wind shear (VWS) is needed to organize storm structure, increasing hailstorm longevity and severity (Dennis & Kumjian, 2017; Markowski & Richardson, 2010; Wallace & Hobbs, 2006; Weisman & Klemp, 1984). In conclusion, strong convective instability, the amount of melting, and storm dynamic structure in response to VWS are three primary conditions that can affect the formation of hailstones that reach the ground, and we aim to find criteria that describe the conditions required to form severe hailstones globally. In this paper, nine environmental parameters which are strongly related to parameterizing these three conditions (Edwards & Thompson, 1998; Giaiotti & Stel, 2006; Phillips et al., 2007; Tang et al., 2019; Xie et al., 2008) were considered to analyze the environmental conditions associated with hailstorms in different parts of the globe.

Within the existing literature, there has been little examination of the environmental typing of severe hailstorms, particularly between different regions. Regionally, climatological studies have revealed the seasonal peak of hailstorm occurrence varies, which suggests that there may be more than one environmental type of hailstorm worldwide. For example, hail occurs in the vicinity of Bangladesh for a short window during the boreal spring (Frisby & Sansom, 1967; Peterson & Mehta, 1981; Williams, 1973) as compared to all year in central Africa (Frisby & Sansom, 1967). It is also unclear the extent to which the dominant convective modes for hailstorms vary in different hotspots. In subtropical South America, the majority of significant hailstorms are not from discrete storms, such as isolated supercells, but rather from organized multicell convection (Bruick et al., 2019). In contrast, the majority of hailstorms producing hail in excess of 5 cm have been found to be associated with supercells in the United States (Blair et al., 2011; Grams et al., 2012; B. T. Smith et al., 2012).

Machine learning offers approaches to explore this through both patterning and clustering. Self-Organizing Maps (SOM; Kohonen, 1982) are a typical artificial intelligence (AI) clustering method that has been successfully utilized in meteorological fields, such as synoptic climatology, climate change analysis, extreme weather, and analysis of rainfall patterns (Y. Liu & Weisberg, 2011). In our work, we apply this methodology to explore if a SOM provides a feasible tool for classifying severe hailstorm environments.

Despite detailed regional studies, the global picture of severe hailstorm environmental characteristics remains unclear. Here we use a uniform hailstorm record derived from a spaceborne precipitation radar (PR) observation and a hailstorm detection algorithm (Ni et al., 2016) to investigate the preferential environment of severe hailstorms with maximum hailstone diameter (MHD) greater than 1.9 cm, ranging from the tropics to temperate zones. We further demonstrate that there are five common types of environmental conditions that appear to favor the formation of severe hailstorms using the SOM clustering method. By leveraging known relationships with environmental conditions, differences in hailstone embryos and the convective modes between these types are investigated.

2. Data and Methods

2.1. Satellite Detected Hail Database

We used a hailstorm detection algorithm based on the precipitation feature (PF) database of Global Precipitation Measurement Core Observatory satellite (GPM) PR measurements (C. Liu et al., 2008; Ni et al., 2016) from April 2014 to March 2021. The algorithm is an event-based method that uses the vertical characteristics of radar reflectivity and uses a threshold value for hail wherein the 44-dBZ echo top temperature is $<-22°C$. To filter snowstorms with solid precipitation, we also use a threshold of surface temperature $>10°C$ (G. Liu, 2008). Based

Table 1
Environmental Parameters Used in the Study

Parameter	Full name	Units
Parameters for clustering		
MUCAPE	Most unstable convective available potential energy	J kg^{-1}
MUCIN	Most unstable convective inhibition	J kg^{-1}
PW	Precipitable water	mm
SHR06	0–6 km bulk shear	m s^{-1}
Hlift	Height of lifting parcel with MUCAPE	m[a]
FLH	Height of 0°C isotherm	m mean sea level (MSL)
Hmelt	Height interval between FLH and terrain height	m
HGZ	Height interval between −30°C and −10°C isotherm	m
Hterrain	terrain height	m MSL
Parameters for sounding schematic		
Tlift	Temperature of lifting parcel with MUCAPE	°C
HLCL/TLCL	Height/temperature of Lifting Condensation Level (LCL)	m $°C^{-1}$
HLFC/TLFC	Height/temperature of Level of Free Convection (LFC)	m $°C^{-1}$
Normalized MUCAPE	MUCAPE divided by the depth of the layer where CAPE is present	m s^{-2}

[a]In this paper, the unit of height refers to *m above ground level* unless otherwise specified.

on this methodology, we identify 14,297 global possible severe hailstorm events with MHD greater than 1.9 cm (Figure S1 in Supporting Information S1) at the surface over land. Although the algorithm is derived based on the Tropical Rainfall Measuring Mission satellite, the skill scores and spatial distribution of GPM detected hail reports suggest that the application is equally valid (Ni et al., 2017).

2.2. Environmental Profiles

Environmental atmospheric profiles related to severe hailstorm events were calculated using the hourly data on pressure and single levels data from the fifth-generation atmospheric reanalysis of the global climate from the European Centre for Medium-Range Weather Forecasts Reanalysis 5 (ERA5) data set (Hersbach et al., 2020) by the Sounding and Hodograph Analysis and Research Program in Python (SHARPpy; Blumberg et al., 2017).

2.3. Definition of Hailstorm Types

We considered nine parameters (Table 1) that are highly associated with the occurrence of hailstorms to define types. These variables belong to three different aspects influencing hail production, convective instability (most unstable CAPE (MUCAPE), most unstable convective inhibition (MUCIN), precipitable water (PW)), storm dynamics and structure (vertical bulk wind shear over between the surface and 6 km mean sea level (SHR06), most unstable lifted parcel height (Hlift)), the effects of melting (freezing level height (FLH), melting zone (Hmelt), hail growth zone (HGZ)), and terrain height (Hterrain). Because the calculation of CAPE is sensitive to fluctuations in the surface moisture and boundary layer condition, we use MUCAPE to overcome this issue (Allen et al., 2011). From the full set of PR hail detections, a subset of 12,256 representative soundings was selected to focus on the respective classes with an acceptable parameter range capable of reflecting severe hailstorms: MUCAPE $\geq$200 J kg^{-1} and lower than the value of the 75 percentile plus 1.5 times the interquartile range (Blanchard, 1998). Similar to prior work (Allen et al., 2011; Brooks et al., 2003), we assume that the largest or smallest values are a reflection of potential outliers, which may reflect poor or contaminated proximity soundings. Following standard practices, prior to clustering all parameters were min-max normalized in preparation for use in the SOM (Tambouratzis & Tambouratzis, 2008).

SOM was selected as a typical unsupervised AI clustering method to identify similar global hailstorm environments. Six widely used internal indexes were used to validate the selection of cluster partitions by considering the

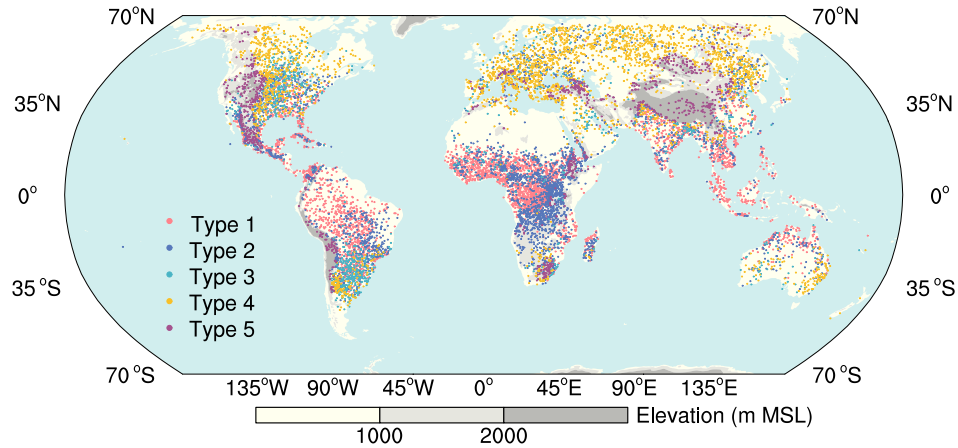

Figure 1. Global distribution of five types severe hailstorms centroid location. The dot colors represent hailstorm types based on environmental similarity as clustering outputs. The topography was divided into three categories according to Hterrain: plain (<1,000 m MSL), foothills (1,000–2,000 m MSL), plateau, and mountains (>2,000 m MSL). Black boxes delineate the respective hot spots for each identified type.

inter-cluster similarity and intra-cluster similarity (Figure S2 in Supporting Information S1). We set nine cluster number options from 2 to 10 and repeated clustering through 500 cross-validations with each cluster option by SOM. Based on analysis of these six metrics and reduction of uncertainty, this led to the conclusion that five clusters was the optimal choice to balance the compactness and separation.

3. Results

3.1. The Global Distribution for Five Types of Potential Severe Hailstorms

The clustering approach identifies five types of severe hailstorms globally with clear hotspots for each type (Figure 1). The first type is concentrated in tropical latitudes across flat plains (Figure 2i), for example, the Congo Basin, the Amazon, Southeast Asia, and monsoonal parts of the sub-continent and northern Australia. A second type also falls in these latitudes at higher altitudes associated with significant orography compared to the first type (Figure 2i). The hotspots of the third type are located in the mid-latitude plains regions of the various regions known to be commonly associated with hail. The fourth cluster type occurs preferentially in high-latitude plains of the Northern Hemisphere, outside a small area of the southern tip of South America. Finally, the fifth type is most prevalent in midlatitude elevated terrain, including the Tibetan Plateau, the Highveld plateau of South Africa, and along the Continental Divides of the Americas.

The seasonal cycle and diurnal cycle of these hailstorm types are analyzed in Figure S3 in Supporting Information S1. In both hemispheres, the maximum frequency occurs during the warm season for all types of hailstorms for the annual cycle. There is a broad peak between 13:00 and 18:00 Local Solar Time (LST) for the diurnal cycle, with types 1, 2, 4, 5 corresponding to earlier in the period and declining nocturnally. In contrast, type 3 storms have less of a diurnal peak and are persistent into the nocturnal hours, which given the stronger VWS may be associated with supercellular or organized storms that can continue into the early morning hours (e.g., Bruick et al., 2019; Bunkers et al., 2006), a signal also seen within regional hail observations (Allen & Tippett, 2015). Both the seasonal cycle and the diurnal cycle are consistent with previous local studies (Allen & Tippett, 2015; Cecil & Blankenship, 2012; Li et al., 2018; Mezher et al., 2012; Punge & Kunz, 2016). The seasonal spatial distribution is also analyzed (Figure S4 in Supporting Information S1). The dominant hailstorm type varies with seasons in some hotspots, such as the central contiguous United States and southern Africa (further discussed in the Supporting Information S1). In spring and autumn, hailstorms concentrate zonally closer to the equator. During the respective hemispheric summers, when the environmental temperature warms and moisture becomes abundant favoring severe convection, the hotspots shift to higher latitudes and elevated terrain.

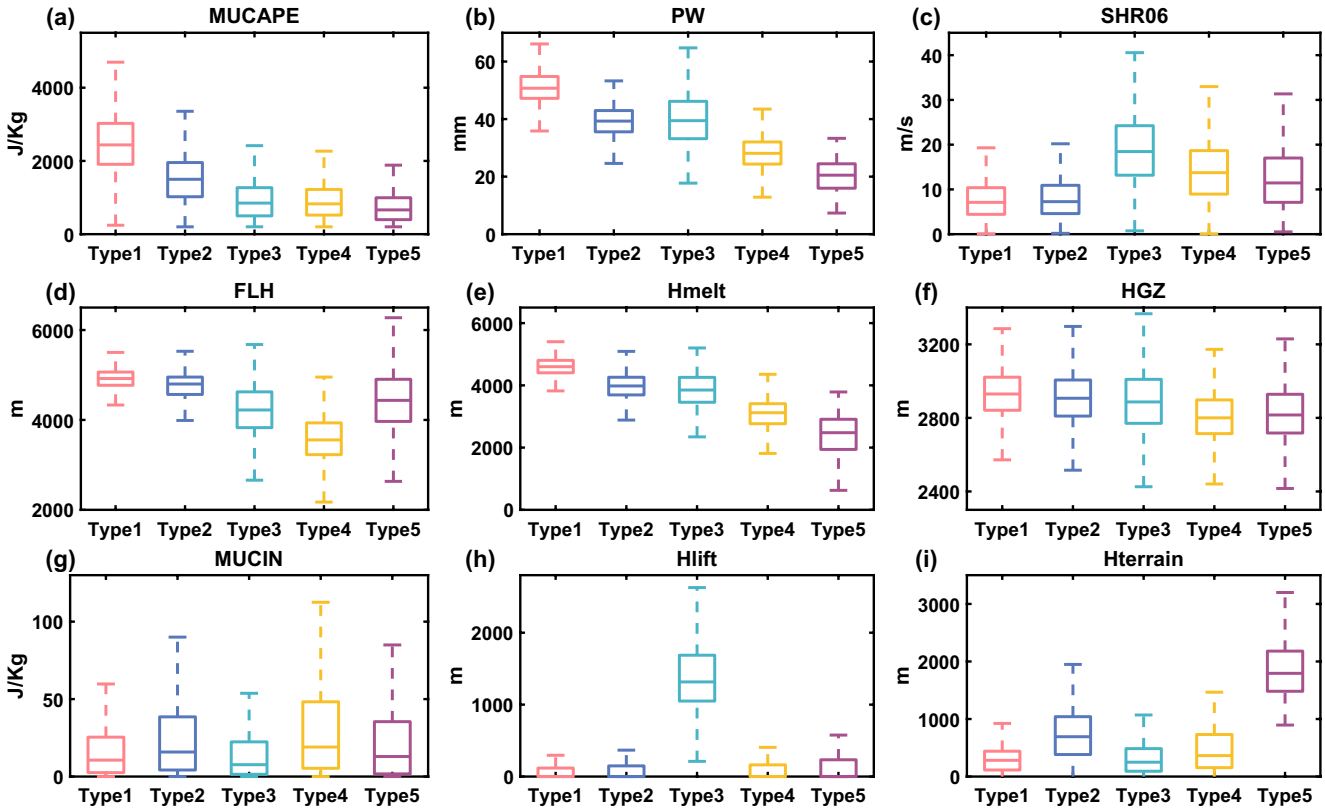

Figure 2. Box-and-whisker plots of most unstable CAPE (MUCAPE; J kg^{-1}), precipitable water (PW; mm), SHR06 (m s^{-1}), freezing level height (FLH; m MSL), Hmelt (m), hail growth zone (HGZ; m), most unstable convective inhibition (MUCIN; J kg^{-1}), Hlift (m), Hterrain (m MSL) for five clusters. The band inside the box is the median, the boxes span the 25th–75th percentiles, while the whiskers extend to the two-tailed 99% confidence interval of the sample to reflect outliers.

3.2. Characteristics of the Five Hailstorm Environments

Analyzing parameters for the five types illustrates substantive environmental differences (Figure 2). A decreasing magnitude of MUCAPE and PW is observed from type 1 to type 5 hailstorm environment characteristics. This reflects relative distance from the tropics (and thus reduced temperature and available moisture) or increasing altitude. Type 3 is characterized by the highest VWS compared to the other four types. It also highlights that storm dynamic structure is the dominant condition for at least one of the severe hailstorm environment types.

Considering the mean values of environmental parameters, the MUCAPE is 2,517.3, 1,524.5, 1,026.9, 950.7, 795.1 J kg^{-1} for types 1–5, respectively (Figure 2a). Corresponding to this decrease, PW is 51.3, 39.2, 40.1, 28.3, 20.5 mm for each type (Figure 2b). Physically, the first two types represent abundant moist and unstable environments characterized by the warm atmospheric temperatures of the tropics. For types 3–5, two factors compensate for the relative decrease in instability: stronger VWS or lower rates of melting. The first two types are characterized by low SHR06, with the mean values of 7.8 and 8.1 m s^{-1}, respectively (Figure 2c). The third type corresponds to an optimal combination of high SHR06 with 19.0 m s^{-1}. This large VWS is largely a function of the regional concentrations of this type within the belts of mid-latitude westerly jet streams in both hemispheres. The net result of this stronger VWS is the convective organization, with enhanced residence within the optimal hail growth zone before falling (Dennis & Kumjian, 2017; Heymsfield, 1983; Kumjian & Lombardo, 2020). Somewhat surprisingly, the SHR06 of the fourth and fifth types are more moderate with 14.3 and 12.4 m s^{-1} on average, reflecting moderately organized storms. Even though the moisture, convective instability, and VWS are not as favorable for the last two types, the lower depth of melting means more severe hailstones reach the surface (Brimelow et al., 2017; Prein & Heymsfield, 2020). One indicator of melting is FLH (Figure 2d), which determines the depth of the atmosphere that is above freezing. The higher FLH reflects hailstones will have more time to melt. However, FLH measures the height above mean sea level, which poses difficulty to compare melting process above varying terrain. In comparison, Hmelt (Figure 2e) is a better indicator, which measures the

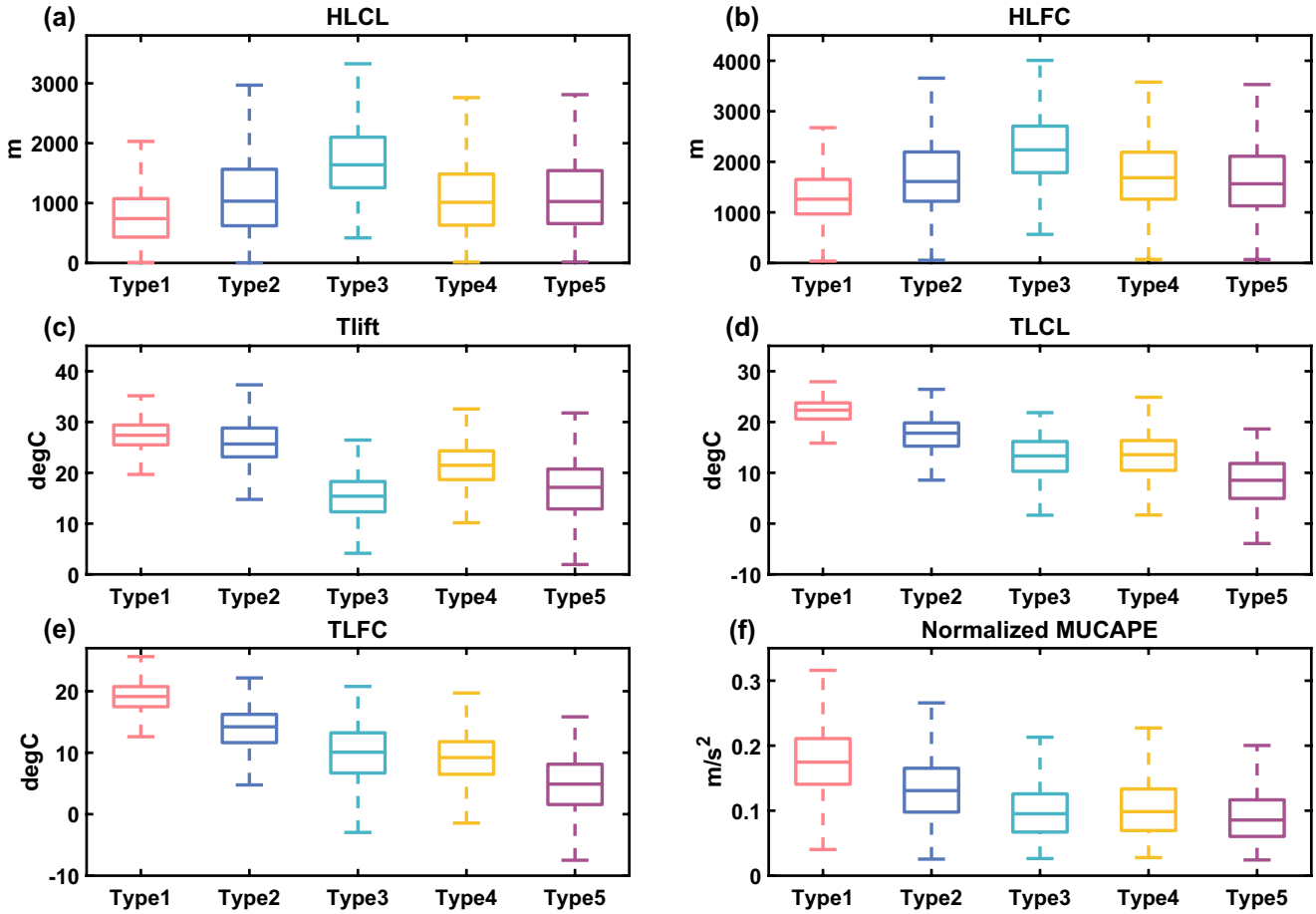

Figure 3. As in Figure 2, but for the HLCL, HLFC (m), Tlift, TLCL, TLFC (°C), Normalized MUCAPE (m s^{-2}).

height above ground level. The low Hmelt means the low surface temperatures through either increasing latitude or altitude. Intriguingly, both HGZ (Figure 2f) and MUCIN (Figure 2g) show a reduced capacity to distinguish between these types.

The mean value of the Hlift (Figure 2h) is also substantially different for type 3 (~1,400 m) contrasting near the surface (~120 m) for the other four types. This suggests that the third type are more likely to be associated with elevated convection (Colman, 1990). We hypothesize that this may be a reflection of the formation of hailstorms at the exit regions of nocturnal low-level jets (e.g., Allen & Tippett, 2015; Bunkers et al., 2006) or lower tropospheric gravity waves (Wilson et al., 2018), which can produce elevated but organized storms.

This suggests that the different global severe hailstorm environmental characteristics reflect a consistent relationship, balancing between unstable conditions, less amount of melting through either lower surface temperature or elevation, and the pressure-gradient updraft strengthening of storm organization through VWS.

3.3. Environmental Sounding Schematics for 5 Types

Based on the mean value of environmental parameters in Figure 3, schematic idealized soundings for five types of severe hailstorms are determined (Figure 4). The vertical accelerations are strongly associated with the buoyancy distribution, which is characterized by Normalized MUCAPE (Blanchard, 1998; Huang et al., 2020). Thus, the growth potential of convective clouds of the first two type is larger than the other three environmental conditions (Figure 3f).

Based on the relationship between the spectrum of storm convective modes and the SHR06 as in Markowski and Richardson (2010), the storm types of each of the environmental types are classified as single cells, multicells,

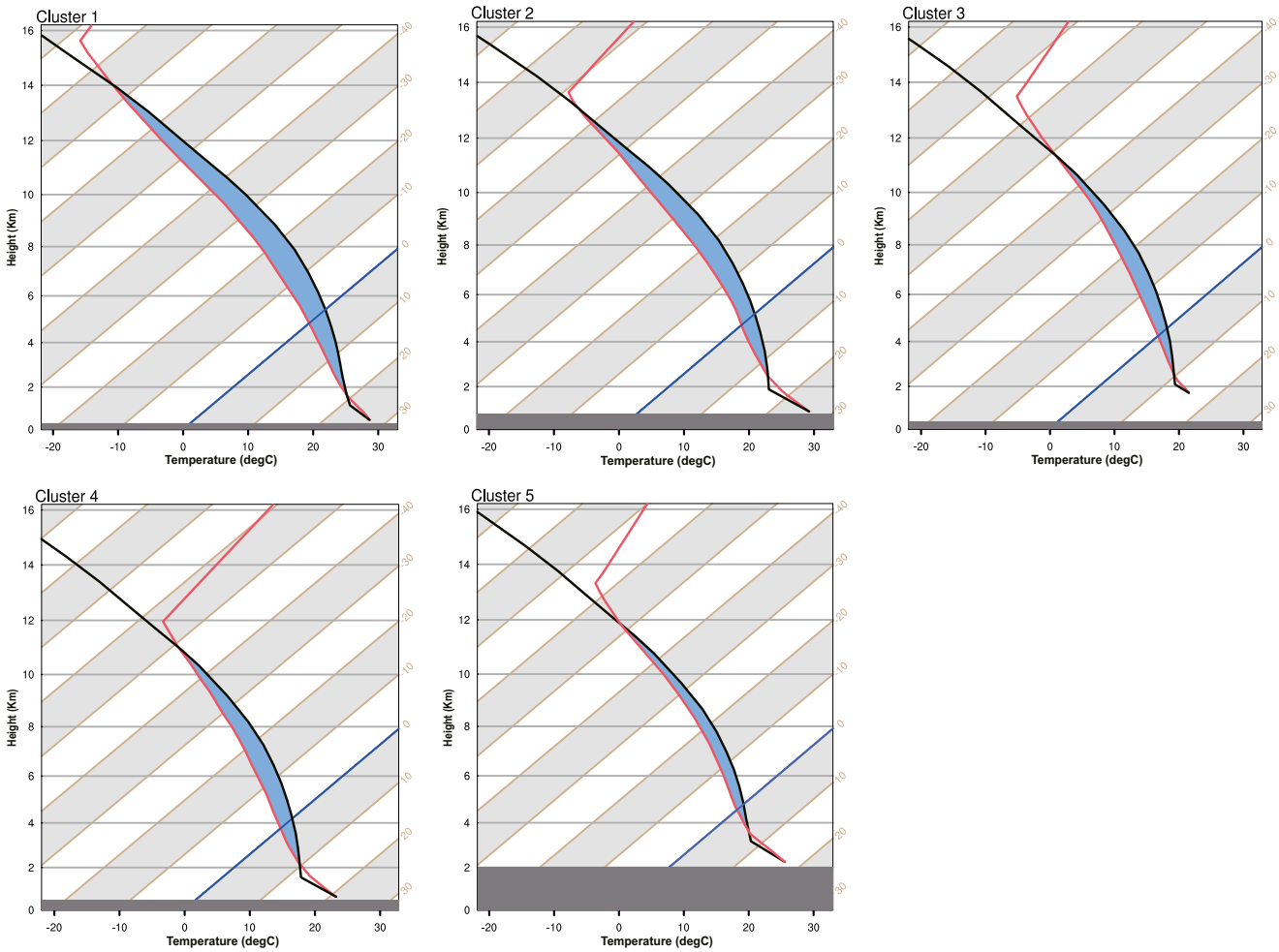

Figure 4. Schematic representation of the five hailstorm environmental types. Isobars (labeled in height (Km)) are light gray and isotherms (labeled in temperature (°C)) are tan. The red line is the temperature profile and the black line is the trace of a parcel that ascends dry adiabatically until saturation then moist adiabatically. Hterrain is marked by dark gray shading.

and supercells. The mean values of SHR06 for the respective types suggest that the first two types are likely to be associated with single cells or weakly organized convection. The third type with strong and deep VWS are more likely to be supercell storms or other strongly organized hybrids (Thompson et al., 2012), while the fourth and fifth likely range between multi-cells or marginal supercells. The significant differences of these types are reflected in their distribution over the respective continents.

The thermal differences across the types also likely have an impact on the dominant hailstone embryo form in different hailstorm types. Referring to Knight (1981), hailstone embryo type is associated with the temperature of the cloud base. Specifically, for cloud base temperatures warmer than 10°C, embryos are more likely to be frozen-drops, whereas graupel embryos tend to dominate when cloud bases are cooler than 10°C. Based on the composite characteristics we can therefore infer that the embryo type of the first four types is more likely to be frozen droplets. For the fifth type, hailstone embryos are more likely to be graupel, which reflects observations over high-latitude plains, plateaus, and mountains (Cecil & Blankenship, 2012; Makitov et al., 2017; K. L. Rasmussen et al., 2014; S. B. Smith et al., 1998). As embryo type can vary for a given region as a function of season, further investigation of this potential relationship is necessary.

4. Summary and Discussion

Leveraging a combination of satellite detections of hail, environmental profiles, and a SOM classification approach, we for the first time demonstrate global differences in five distinct environmental clusters producing hail storms. The distinguishing differences between the environmental parameters of these classes paired with composite soundings, and the non-uniform distribution of these events both spatially and in terms of seasonal peak of occurrence, implies that a single approach that only reflects the conditions favorable to a single hailstorm type is not sufficient to understand global severe hailstorm occurrence. Given recent studies exploring the response of hail to climate change (Brimelow et al., 2017; Raupach et al., 2021), this suggests that to understand the response of these storms, a variety of processes and mechanisms must be considered and changes monitored over different regions.

While these results reflect a promising step forward, we note that severe hailstorms detected using PR are identified based on vertical structural reflectivity characteristics of convective clouds. Although these measurements have been well-calibrated to large hail reports over the United States and China, this is not the case for all regions nor latitudes (Ni et al., 2016). There are two challenges to validate the satellite-detected hailstorm with surface hail observations. One challenge is that there are very few surface hail records in tropical regions. The other is that some of the literature on high-latitude hail observations is in national languages other than English. While the limited surface observations in these regions do verify the probability of severe hailstorms occurrence detected by satellite, for example, the spatial distribution of hail reporting records over Africa (Dyson et al., 2021; Frisby & Sansom, 1967) and Russia (Abshaev et al., 2009) is consistent with Figure 1. By establishing a threshold where convection has a high likelihood of being a severe hailstorm (MHD>1.9 cm), this provides a feasible method to understand the sounding structure and environmental characteristics where direct surface observations are sparse. Together with AI techniques, this has offered an unprecedented insight into the environments of global hailstorms.

Future work to explore these environments using hail growth simulations by HAILCAST is planned to better validate the global spatial distribution and extend the dynamic explanations for hailstone occurrence.

Data Availability Statement

The GPM PF database is available at http://atmos.tamucc.edu/trmm/ in the directory/trmm/data/gpm/. The ERA5 reanalysis data set is downloaded from https://cds.climate.copernicus.eu/cdsapp#!/dataset/reanalysis-era5-pressure-levels?tab=overview and https://cds.climate.copernicus.eu/cdsapp#!/dataset/reanalysis-era5-single-levels?tab=overview. The SHARPpy is available at https://sharppy.github.io/SHARPpy/index.html and the related paper can be achieved at https://doi.org/10.1175/BAMS-D-15-00309.1.

Acknowledgments
The authors would like to thank Chuntao Liu from the Department of Physical and Environmental Sciences at Texas A&M University for providing and updating PF database. The authors acknowledge excellent comments from two anonymous reviewers. Z. Zhou and Q. Zhang acknowledge funding support from the National Nature Science Foundation of China (42030607 and 41875052). J. Allen acknowledges funding support from the National Science Foundation (AGS-1945286).

References

Abshaev, M., Malkarova, A., & Borisova, N. (2009). Zoning of the territory by hail hazard. *Tech. Rep., RD*, *5237*, 722–439. https://doi.org/10.1127/0941-2948/2010/0452

Adams-Selin, R. D., & Ziegler, C. L. (2016). Forecasting hail using a one-dimensional hail growth model within WRF. *Monthly Weather Review*, *144*(12), 4919–4939. https://doi.org/10.1175/mwr-d-16-0027.1

Allen, J. T., Giammanco, I. M., Kumjian, M. R., Jurgen Punge, H., Zhang, Q., Groenemeijer, P., et al. (2020). Understanding hail in the Earth system. *Reviews of Geophysics*, *58*(1), e2019RG000665. https://doi.org/10.1029/2019rg000665

Allen, J. T., Karoly, D. J., & Mills, G. A. (2011). A severe thunderstorm climatology for Australia and associated thunderstorm environments. *Australian Meteorological and Oceanographic Journal*, *61*(3), 143–158. https://doi.org/10.22499/2.6103.001

Allen, J. T., & Tippett, M. K. (2015). The characteristics of United States hail reports: 1955–2014. *Electronic Journal of Severe Storms Meteorology*, *10*, 1–31. https://ejssm.org/archives/wp-content/uploads/2021/09/vol10-3.pdf

Allen, J. T., Tippett, M. K., & Sobel, A. H. (2015). An empirical model relating U.S. monthly hail occurrence to large-scale meteorological environment. *Journal of Advances in Modeling Earth Systems*, *7*(1), 226–243. https://doi.org/10.1002/2014ms000397

Blair, S. F., Deroche, D. R., Boustead, J. M., Leighton, J. W., Barjenbruch, B. L., & Gargan, W. P. (2011). A radar-based assessment of the detectability of giant hail. *E-Journal of Severe Storms Meteorology*, *6*(7), 1–30. Retrieved from https://ejssm.org/archives/wp-content/uploads/2021/09/vol6-7.pdf

Blanchard, D. O. (1998). Assessing the vertical distribution of convective available potential energy. *Weather and Forecasting*, *13*(3), 870–877. https://doi.org/10.1175/1520-0434(1998)013<0870:atvdoc>2.0.co;2

Blumberg, W. G., Halbert, K. T., Supinie, T. A., Marsh, P. T., Thompson, R. L., & Hart, J. A. (2017). SHARPpy: An open-source sounding analysis toolkit for the atmospheric sciences. *Bulletin of the American Meteorological Society*, *98*(8), 1625–1636. https://doi.org/10.1175/BAMS-D-15-00309.1

Brimelow, J. C., Burrows, W. R., & Hanesiak, J. M. (2017). The changing hail threat over North America in response to anthropogenic climate change. *Nature Climate Change*, *7*(7), 516–522. https://doi.org/10.1038/nclimate3321

Brimelow, J. C., Reuter, G. W., & Poolman, E. R. (2002). Modeling maximum hail size in Alberta thunderstorms. *Weather and Forecasting*, *17*(5), 1048–1062. https://doi.org/10.1175/1520-0434(2002)017<1048:mmhsia>2.0.co;2

Brooks, H. E., Lee, J. W., & Craven, J. P. (2003). The spatial distribution of severe thunderstorm and tornado environments from global reanalysis data. *Atmospheric Research*, *67*(68), 73–94. https://doi.org/10.1016/s0169-8095(03)00045-0

Bruick, Z. S., Rasmussen, K. L., & Cecil, D. J. (2019). Subtropical South American hailstorm characteristics and environments. *Monthly Weather Review*, *147*(12), 4289–4304. https://doi.org/10.1175/MWR-D-19-0011.1

Bunkers, M. J., Hjelmfelt, M. R., & Smith, P. L. (2006). An observational examination of long-lived supercells. Part I: Characteristics, evolution, and demise. *Weather and Forecasting*, *21*(5), 673–688. https://doi.org/10.1175/WAF949.1

Cecil, D. J., & Blankenship, C. B. (2012). Toward a global climatology of severe hailstorms as estimated by satellite passive microwave imagers. *Journal of Climate*, *25*(2), 687–703. https://doi.org/10.1175/jcli-d-11-00130.1

Colman, B. R. (1990). Thunderstorms above frontal surfaces in environments without positive CAPE. Part I: A climatology. *Monthly Weather Review*, *118*(5), 1103–1122. https://doi.org/10.1175/1520-0493(1990)118<1103:tafsie>2.0.co;2

Czernecki, B., Taszarek, M., Marosz, M., Półrolniczak, M., Kolendowicz, L., Wyszogrodzki, A., & Szturc, J. (2019). Application of machine learning to large hail prediction—The importance of radar reflectivity, lightning occurrence and convective parameters derived from ERA5. *Atmospheric Research*, *227*, 249–262. https://doi.org/10.1016/j.atmosres.2019.05.010

Dennis, E. J., & Kumjian, M. R. (2017). The impact of vertical wind shear on hail growth in simulated supercells. *Journal of the Atmospheric Sciences*, *74*(3), 641–663. https://doi.org/10.1175/JAS-D-16-0066.1

Dessens, J., Berthet, C., & Sanchez, J. L. (2015). Change in hailstone size distributions with an increase in the melting level height. *Atmospheric Research*, *158–159*, 245–253. https://doi.org/10.1016/j.atmosres.2014.07.004

Dyson, L. L., Pienaar, N., Smit, A., & Kijko, A. (2021). An ERA-Interim HAILCAST hail climatology for southern Africa. *International Journal of Climatology*, *41*(1), 262–277. https://doi.org/10.1002/joc.6619

Edwards, R., & Thompson, R. L. (1998). Nationwide comparisons of hail size with WSR-88D vertically integrated liquid water and derived thermodynamic sounding data. *Weather and Forecasting*, *13*(2), 277–285. https://doi.org/10.1175/1520-0434(1998)013<0277:ncohsw>2.0.co;2

Frisby, E. M., & Sansom, H. W. (1967). Hail incidence in the tropics. *Journal of Applied Meteorology and Climatology*, *6*(2), 339–354. https://doi.org/10.1175/1520-0450(1967)006<0339:hiitt>2.0.co;2

Giaiotti, D. B., & Stel, F. (2006). The effects of environmental water vapor on hailstone size distributions. *Atmospheric Research*, *82*(1–2), 455–462. https://doi.org/10.1016/j.atmosres.2006.02.002

Grams, J. S., Thompson, R. L., Snively, D. V., Prentice, J. A., Hodges, G. M., & Reames, L. J. (2012). A climatology and comparison of parameters for significant tornado events in the United States. *Weather and Forecasting*, *27*(1), 106–123. https://doi.org/10.1175/WAF-D-11-00008.1

Groenemeijer, P. H., & Delden, A. v. (2007). Sounding-derived parameters associated with large hail and tornadoes in the Netherlands. *Atmospheric Research*, *83*(2), 473–487. https://doi.org/10.1016/j.atmosres.2005.08.006

Gutierrez, R. E., & Kumjian, M. R. (2021). Environmental and radar characteristics of Gargantuan hail-producing storms. *Monthly Weather Review*, *1*, 2523–2538. https://doi.org/10.1175/MWR-D-20-0298.1

Hersbach, H., Bell, B., Berrisford, P., Hirahara, S., Horányi, A., Muñoz-Sabater, J., et al. (2020). The ERA5 global reanalysis. *Quarterly Journal of the Royal Meteorological Society*, *146*(730), 1999–2049. https://doi.org/10.1002/qj.3803

Heymsfield, A. J. (1983). Case study of a halistorm in Colorado. Part IV: Graupel and hail growth mechanisms deduced through particle trajectory calculations. *Journal of the Atmospheric Sciences*, *40*(6), 1482–1509. https://doi.org/10.1175/1520-0469(1983)040<1482:csoahi>2.0.co;2

Huang, Y., Wang, X., Pei, J., & Ma, Y. (2020). Mesoscale characteristics of a rare severe hailstorm event. *Meteorology and Atmospheric Physics*, *132*(2), 159–170. https://doi.org/10.1007/s00703-019-00680-x

Johnson, A., & Sugden, K. (2014). Evaluation of sounding-derived thermodynamic and wind-related parameters associated with large hail events. *E-Journal of Severe Storms Meteorology*, *9*(5). https://ejssm.org/archives/wp-content/uploads/2021/09/vol9-5.pdf

Kahraman, A., Tilev-Tanriover, Ş., Kadioglu, M., Schultz, D. M., & Markowski, P. M. (2016). Severe hail climatology of Turkey. *Monthly Weather Review*, *144*(1), 337–346. https://doi.org/10.1175/mwr-d-15-0337.1

Knight, C. A., & Knight, N. C. (1974). Drop freezing in clouds. *Journal of the Atmospheric Sciences*, *31*(4), 1174–1176. https://doi.org/10.1175/1520-0469(1974)031<1174:dfic>2.0.co;2

Knight, N. C. (1981). The Climatology of hailstone embryos. *Journal of Applied Meteorology and Climatology*, *20*(7), 750–755. https://doi.org/10.1175/1520-0450(1981)020<0750:tcohe>2.0.co;2

Kohonen, T. (1982). Self-organized formation of topologically correct feature maps. *Biological Cybernetics*, *43*(1), 59–69. https://doi.org/10.1007/BF00337288

Kumjian, M. R., & Lombardo, K. (2020). A hail growth trajectory model for exploring the environmental controls on hail size: Model physics and idealized tests. *Journal of the Atmospheric Sciences*, *77*(8), 2765–2791. https://doi.org/10.1175/JAS-D-20-0016.1

Li, M., Zhang, D.-L., Sun, J., & Zhang, Q. (2018). A statistical analysis of hail events and their environmental conditions in China during 2008–15. *Journal of Applied Meteorology and Climatology*, *57*(12), 2817–2833. https://doi.org/10.1175/jamc-d-18-0109.1

Liu, C., Zipser, E. J., Cecil, D. J., Nesbitt, S. W., & Sherwood, S. (2008). A cloud and precipitation feature database from nine years of TRMM observations. *Journal of Applied Meteorology and Climatology*, *47*(10), 2712–2728. https://doi.org/10.1175/2008JAMC1890.1

Liu, G. (2008). Deriving snow cloud characteristics from CloudSat observations. *Journal of Geophysical Research*, *113*(D8), D00A09. https://doi.org/10.1029/2007JD009766

Liu, Y., & Weisberg, R. H. (2011). A review of self-organizing map applications in meteorology and oceanography. In J. I. Mwasiagi (Ed.), *Self-organizing maps: Applications and novel algorithm design* (pp. 253–272). IntechOpen. https://doi.org/10.5772/13146

Ma, R., Feng, S., Jin, S., Sun, J., Fu, S., Sun, S., & Han, H. (2021). Statistical characteristics and environmental conditions of the warm-season severe convective events over North China. *Atmosphere*, *12*(1), 52. https://doi.org/10.3390/atmos12010052

Mahoney, K. (2020). Extreme hail storms and climate change: Foretelling the future in tiny, turbulent crystal balls? *Bulletin of the American Meteorological Society*, *101*(1), S17–S22. https://doi.org/10.1175/BAMS-D-19-0233.1

Mahoney, K., Alexander, M. A., Thompson, G., Barsugli, J. J., & Scott, J. D. (2012). Changes in hail and flood risk in high-resolution simulations over Colorado's mountains. *Nature Climate Change*, *2*(2), 125–131. https://doi.org/10.1038/nclimate1344

Makitov, V. S., Inyukhin, V. S., Kalov, H. M., & Kalov, R. H. (2017). Radar research of hailstorm formation and development over the central part of Northern Caucasus (Russia). Organization and main results of the regional hail suppression projects. *Natural Hazards*, *88*(1), 253–272. https://doi.org/10.1007/s11069-016-2433-7

Manzato, A. (2013). Hail in Northeast Italy: A neural network ensemble forecast using sounding-derived indices. *Weather and Forecasting*, *28*(1), 3–28. https://doi.org/10.1175/WAF-D-12-00034.1

Markowski, P., & Richardson, Y. (2010). Organization of isolated convection. In *Mesoscale meteorology in midlatitudes* (pp. 201–244). John Wiley & Sons, Ltd. Retrieved from https://onlinelibrary.wiley.com/doi/abs/10.1002/9780470682104.ch8

Mezher, R. N., Doyle, M., & Barros, V. (2012). Climatology of hail in Argentina. *Atmospheric Research*, *114–115*, 70–82. https://doi.org/10.1016/j.atmosres.2012.05.020

Nelson, S. P. (1983). The influence of storm flow structure on hail growth. *Journal of the Atmospheric Sciences*, *40*(8), 1965–1983. https://doi.org/10.1175/1520-0469(1983)040<1965:tiosfs>2.0.co;2

Nelson, S. P. (1987). The hybrid multicellular–Supercellular storm—An efficient hail producer. Part II. General characteristics and implications for hail growth. *Journal of the Atmospheric Sciences*, *44*(15), 2060–2073. https://doi.org/10.1175/1520-0469(1987)044<2060:thmseh>2.0.co;2

Ni, X., Liu, C., Cecil, D. J., & Zhang, Q. (2017). On the detection of hail using satellite passive microwave radiometers and precipitation radar. *Journal of Applied Meteorology and Climatology*, *56*(10), 2693–2709. https://doi.org/10.1175/jamc-d-17-0065.1

Ni, X., Liu, C., Zhang, Q., & Cecil, D. J. (2016). Properties of hail storms over China and the United States from the tropical rainfall measuring mission. *Journal of Geophysical Research: Atmosphere*, *121*(20), 12031–12044. https://doi.org/10.1002/2016JD025600

Peterson, R. E., & Mehta, K. C. (1981). Climatology of tornadoes of India and Bangladesh. *Archives for Meteorology, Geophysics, and Bioclimatology, Series B*, *29*(29), 345–356. https://doi.org/10.1007/BF02263310

Phillips, V. T. J., Pokrovsky, A., & Khain, A. (2007). The influence of time-dependent melting on the dynamics and precipitation production in maritime and continental storm clouds. *Journal of the Atmospheric Sciences*, *64*(2), 338–359. https://doi.org/10.1175/jas3832.1

Prein, A. F., & Heymsfield, A. J. (2020). Increased melting level height impacts surface precipitation phase and intensity. *Nature Climate Change*, *10*(8), 771–776. https://doi.org/10.1038/s41558-020-0825-x

Prein, A. F., & Holland, G. J. (2018). Global estimates of damaging hail hazard. *Weather and Climate Extremes*, *22*, 10–23. https://doi.org/10.1016/j.wace.2018.10.004

Pruppacher, H. R., & Klett, J. D. (1997). *Microphysics of clouds and precipitation* (p. 954). Oxford University Press.

Púčik, T., Groenemeijer, P., Rýva, D., & Kolář, M. (2015). Proximity soundings of severe and nonsevere thunderstorms in Central Europe. *Monthly Weather Review*, *143*(12), 4805–4821. https://doi.org/10.1175/MWR-D-15-0104.1

Punge, H. J., & Kunz, M. (2016). Hail observations and hailstorm characteristics in Europe: A review. *Atmospheric Research*, *176–177*, 159–184. https://doi.org/10.1016/j.atmosres.2016.02.012

Rasmussen, K. L., Zuluaga, M. D., & Houze, R. A. (2014). Severe convection and lightning in subtropical South America. *Geophysical Research Letters*, *41*(20), 7359–7366. https://doi.org/10.1002/2014gl061767

Rasmussen, R. M., & Heymsfield, A. J. (1987). Melting and shedding of Graupel and Hail. Part I: Model physics. *Journal of the Atmospheric Sciences*, *44*(19), 2754–2763. https://doi.org/10.1175/1520-0469(1987)044<2754:masoga>2.0.co;2

Raupach, T. H., Martius, O., Allen, J. T., Kunz, M., Lasher-Trapp, S., Mohr, S., et al. (2021). The effects of climate change on hailstorms. *Nature Reviews Earth & Environment*, *2*(3), 213–226. https://doi.org/10.1038/s43017-020-00133-9

Seneviratne, S. I., Nicholls, N., Easterling, D., Goodess, C. M., Kanae, S., Kossin, J., et al. (2012). Changes in climate extremes and their impacts on the natural physical environment. In C. B. Field, V. Barros, T. F. Stocker, & Q. Dahe (Eds.), *Managing the risks of extreme events and disasters to advance climate change adaptation* (pp. 109–230). Cambridge University Press. Retrieved from https://www.cambridge.org/core/product/identifier/CBO9781139177245A030/type/book_part

Smith, B. T., Thompson, R. L., Grams, J. S., Broyles, C., & Brooks, H. E. (2012). Convective modes for significant severe thunderstorms in the contiguous United States. Part I: Storm classification and climatology. *Weather and Forecasting*, *27*(5), 1114–1135. https://doi.org/10.1175/WAF-D-11-00115.1

Smith, S. B., Reuter, G. W., & Yau, M. K. (1998). The episodic occurrence of hail in central Alberta and the Highveld of South Africa: Research note. *Atmosphere-Ocean*, *36*(2), 169–178. https://doi.org/10.1080/07055900.1998.9649610

Tambouratzis, T., & Tambouratzis, G. (2008). Meteorological data analysis using self-organizing maps. *International Journal of Intelligent Systems*, *23*(6), 735–759. https://doi.org/10.1002/int.20294

Tang, B. H., Gensini, V. A., & Homeyer, C. R. (2019). Trends in United States large hail environments and observations. *Npj Climate and Atmospheric Science*, *2*(1), 45. https://doi.org/10.1038/s41612-019-0103-7

Taszarek, M., Allen, J. T., Marchio, M., & Brooks, H. E. (2021). Global climatology and trends in convective environments from ERA5 and rawinsonde data. *Npj Climate and Atmospheric Science*, *4*(1), 35. https://doi.org/10.1038/s41612-021-00190-x

Taszarek, M., Pilguj, N., Allen, J. T., Gensini, V., Brooks, H. E., & Szuster, P. (2021). Comparison of convective parameters derived from ERA5 and MERRA-2 with rawinsonde data over Europe and North America. *Journal of Climate*, *34*(8), 3211–3237. https://doi.org/10.1175/JCLI-D-20-0484.1

Thompson, R. L., Smith, B. T., Grams, J. S., Dean, A. R., & Broyles, C. (2012). Convective modes for significant severe thunderstorms in the contiguous United States. Part II: Supercell and QLCS tornado environments. *Weather and Forecasting*, *27*(5), 1136–1154. https://doi.org/10.1175/WAF-D-11-00116.1

Wallace, J. M., & Hobbs, P. V. (Eds.). (2006). Atmospheric science (second edition) (Vol. 92, 2nd ed., pp. 471–483). Academic Press. https://doi.org/10.1016/B978-0-12-732951-2.50018-1

Weisman, M. L., & Klemp, J. B. (1984). The structure and classification of numerically simulated convective storms in directionally varying wind shears. *Monthly Weather Review*, *112*(12), 2479–2498. https://doi.org/10.1175/1520-0493(1984)112<2479:tsacon>2.0.co;2

Williams, L. (1973). *Studies of the army aviation (V/STOL) environment report no. 8. Hail and its distribution*. ARMY ENGINEER TOPOGRAPHIC LABS FORT BELVOIR VA.

Willis, P. T., & Heymsfield, A. J. (1989). Structure of the melting layer in mesoscale convective system stratiform precipitation. *Journal of the Atmospheric Sciences*, *46*(13), 2008–2025. https://doi.org/10.1175/1520-0469(1989)046<2008:sotmli>2.0.co;2

Wilson, J. W., Trier, S. B., Reif, D. W., Roberts, R. D., & Weckwerth, T. M. (2018). Nocturnal elevated convection initiation of the PECAN 4 July hailstorm. *Monthly Weather Review*, *146*(1), 243–262. https://doi.org/10.1175/MWR-D-17-0176.1

Xie, B., Zhang, Q., & Wang, Y. (2008). Trends in hail in China during 1960–2005. *Geophysical Research Letters*, *35*(13), L13801. https://doi.org/10.1029/2008gl034067

References From the Supporting Information

Barnston, A. G. (1992). Correspondence among the correlation, RMSE, and Heidke forecast verification measures; refinement of the Heidke score. *Weather and Forecasting*, *7*(4), 699–709. https://doi.org/10.1175/1520-0434(1992)007<0699:CATCRA>2.0.CO;2

Calinski, T., & Harabasz, J. (1974). A dendrite method for cluster analysis. *Communications in Statistics - Theory and Methods*, *3*(1), 1–27. https://doi.org/10.1080/03610927408827101

Davies, D. L., & Bouldin, D. W. (1979). A cluster separation measure. *IEEE Transactions on Pattern Analysis and Machine Intelligence*, *PAMI-1*(2), 224–227. https://doi.org/10.1109/TPAMI.1979.4766909

Krzanowski, W. J., & Lai, Y. T. (1988). A criterion for determining the number of groups in a data set using sum-of-squares clustering. *Biometrics*, *44*(1), 23–34. https://doi.org/10.2307/2531893

Liu, N., & Liu, C. (2018). Synoptic environments and characteristics of convection reaching the tropopause over Northeast China. *Monthly Weather Review*, *146*(3), 745–759. https://doi.org/10.1175/MWR-D-17-0245.1

Liu, N., Liu, C., Chen, B., & Zipser, E. (2020). What are the favorable large-scale environments for the highest-flash-rate thunderstorms on Earth? *Journal of the Atmospheric Sciences*, *77*(5), 1583–1612. https://doi.org/10.1175/JAS-D-19-0235.1

Liu, N., Liu, C., & Hayden, L. (2020). Climatology and detection of overshooting convection from 4 years of GPM precipitation radar and passive microwave observations. *Journal of Geophysical Research: Atmosphere*, *125*(7), e2019JD032003. https://doi.org/10.1029/2019JD032003

Rousseeuw, P. J. (1987). Silhouettes: A graphical aid to the interpretation and validation of cluster analysis. *Journal of Computational and Applied Mathematics*, *20*, 53–65. https://doi.org/10.1016/0377-0427(87)90125-7

Strehl, A., & Ghosh, J. (2002). *Relationship-based clustering and cluster ensembles for high-dimensional data mining*. http://hdl.handle.net/2152/967